First-Principles Calculation of the Cu-Li Phase Diagram

Axel van de Walle
Materials Science and Engineering Department,
Northwestern University, Evanston, IL, USA
http://cms.northwestern.edu/avdw
avdw@alum.mit.edu

Zbigniew Moser
Wladyslaw Gasior
I*nstytut Metalurgii i Inżynierii Materiałowej PAN im,*
Aleksandra Krupkowskiego, Poland

Abstact

We present first-principles calculations of the solid-state portion of the Cu-Li phase diagram based on the cluster expansion formalism coupled with the use of (i) bond length-dependent transferable force constants and lattice dynamics calculations to model of vibrational disorder and (ii) lattice gas Monte Carlo simulations to model configurational disorder. These calculations help settle the existence of additional phases in the Cu-Li phase diagram that have been postulated, but not yet clearly established. Our calculations predict the presence of at least one additional phase and the associated predicted phase transitions are consistent with our electrochemical measurements, which exhibit clear plateaus in the electromotive force-composition curve.

1. Introduction

In 1976, Smith and Moser [1] published the thermodynamic assessments of binary lithium alloys using information from the literature, followed by experimental investigations by galvanic cells initiated at the Institute of Metallurgy and Materials Sciences in Kraków in 1981 in cooperation with the University of Saarland in Germany. The following binary systems were studied: Li-Sn [2], Al-Li [3], Li-Zn [4], Li-In [5], Li-Zn [6],Li-Tl [7], Li-Bi [8], Li-Sn [9],Li-Mg [10] and Li-Pb [11]. These studies were extended later to ternary Al-Li-Mg alloys including calorimetric measurements in cooperation with the Max Planck Institute in Stuttgart [12] and to phase diagram calculations of Al-Li-Mg [13] and on Al-Li-Cu [14] systems. In 1998 [14] during the *Thermodynamics of Alloys Conference*, thermodynamic studies of solid Cu-Li alloys from electromotive force (emf) measurements were presented that suggested the existence of intermetallic phases.

Previous phase diagram assessments of Pelton [15] and of Saunders [16] do not indicate the existence of intermetallic phases. In 1996, Borgstedt and Gumiński [17] performed a critical evaluation of previous phase diagram assessments. They indicated that the only experimental thermodynamic data of enthalpies of mixing [18] of liquid alloys based on Cu exhibiting slight exothermic effect (-1.1 kJ/mol) suggests negative deviations from ideal behavior. In addition, taking into account results of Kraus et al. [19] and Old et al.[20] who suggested the formation of Cu_4Li phase, probably formed at the temperature 473-873 K, Borgstedt and Gumiński [17] introduced this phase into a schematic phase diagram of the Cu-Li system based on Pelton's [15]

assessment. It should be noted that estimates of enthalpy of mixing by Miedema et al. [21] yield a much more exothermic effect for the Cu-Li system amounting to –39 kJ/mol.

In this article, we employ first-principles calculations in conjunction with electrochemical measurements to investigate the presence of intermetallic phases in the Cu-Li system. Our findings suggest that the only stable ordered compound above room temperature is the B32 phase at 50 at % Li, which undergoes a second order phase transition into a bcc solid solution around 900K-1200K. Our results also indicate that the previously suggested Cu_4Li phase is probably a Cu-rich bcc solid solution.

2. Methodology

2.1 Computational

All thermodynamics calculations were performed with the Alloy Theoretic Automated Toolkit (ATAT) [22-24] using, as an input, first-principles total energy calculations obtained with the Vienna Ab initio Simulation Package (VASP) [25-26] within the Local Density Approximation (LDA). The energetics of the bcc and fcc phases of the alloy were modeled using the cluster expansion formalism [27-32], in which the configurational dependence of the alloy's energy is represented as a polynomial function of spin-like occupation variables taking the value +1 or -1, depending on the chemical species residing on a given lattice site. The coefficients of this polynomial, called the Effective Custer Interactions (ECI), are determined by a least-squares fit to the energies calculated from first-principles.

An automated algorithm, described in [23], was used to select of the optimal number of terms in the cluster expansion as well as to select the structural energies to be included in the fit.

Figure 1 depicts the database of structural energies, plotted as a function of composition, (top) that were used to obtain the ECI (bottom). The characteristics of the resulting cluster expansions used are summarized in Table 1. While the accuracy of the fit, as measured by the crossvalidation score [23], is quite good for the fcc lattice, the cluster expansion for the bcc lattice appears somewhat less accurate. However, inspection of the residuals of the least-squares fit reveals that most of the prediction error is concentrated in the region 50 at % < x_{Li} < 95 at %, in the unstable portion of the miscibility gap of the bcc phase. The prediction error in the concentration range where the bcc phase is stable is only about 15 meV. These "statistical" errors dominate the numerical precision of the first-principles calculations used as an input, which is of the order of a few meV. This accuracy was obtained by using the "high" precision setting of the VASP code and a *k*-point mesh consisting of no less than 2000 points in the reciprocal cell of the fcc or bcc primitive unit cell.

The cluster expansion enables a very thorough search for the alloy system's ground states, i.e. the stable phases at absolute zero. The ground states of the system were identified using the enumeration method, by calculating formation energies of a large number of ordered structures (containing up to 10 atoms per unit cell) using the cluster expansion and plotting them in the (composition, energy) plane. The structures touching the convex hull of all points are the stable structures at absolute zero, as a function of composition. Of course, this approach can only identify ground states that are superstructures of the lattices given as an input, here bcc and fcc.

In order to account for vibrational degrees of freedom in addition to the configurational degrees of freedom considered above, lattice dynamics calculations [33,34] were used to determine the vibrational free energy of each of the structures employed in the construction of the cluster expansions described above. The resulting temperature-dependent free energies were then used to obtain a temperature-dependent cluster expansion that accounts for vibrational degrees of freedom [34,35].

The vibrational contribution to the free energy was calculated using a hybrid approach. Determining the vibrational free energy difference between the bcc and fcc phases requires a very accurate and computationally intensive method due to the change in coordination, while vibrational free energy differences within the same lattice can be accurately calculated using a simplified method. In light of this observation, the vibrational free energy of pure Li and pure Cu in both the bcc and fcc crystal structures were obtained by constructing a 4^{th} nearest neighbor volume-dependent Born-von Kármán spring model [33,34]. To this effect, the reaction forces induced by small imposed displacements (0.2 Å) were calculated from first-principles and were used to determine the values of all the spring constant tensors via a least-squares fit. The same analysis was carried out after applying isotropic strains of 1,2, and 3% in order to determine the volume dependence of the spring constants, thus permitting the use of the quasi-harmonic approximation [34], which provides free energies that properly account for thermal expansion.

The determination of vibrational free energy differences within the same lattice relies a simplified model based on Length-Dependent Transferable Force Constant (LDTFC) [34,36].

The basic idea is to rely on the observation that bond length is a good predictor of bond stiffness (for a given lattice and a given type of chemical bond). The bond length-bond stiffness relationship can be determined by calculating, from first-principles, the stretching and bending force constants in a few ordered compounds as a function of volume (see Figure 2). Once this relationship is known, the force constants needed for the calculation of the vibrational free energy of a given structure can be predicted solely from the knowledge of its relaxed geometry (which provides the bond lengths).

Finite temperature thermodynamic properties accounting for both configurational and vibrational degrees of freedom were obtained using lattice gas Monte Carlo simulations [37,38] within a grand canonical ensemble, where the alloy's energetics are described by the temperature-dependent cluster expansion constructed above. Free energies were calculated via thermodynamic integration using either internal energy or composition (appropriately scaled by a function of temperature) as the integrand and a low temperature expansion of the free energy was used as the initial conditions for the integration procedure [24]. The temperature-composition phase boundaries associated with first-order transition were located using the standard common tangent construction while the location of the second-order transitions were determined by tracking a peak in the heat capacity.

Since modeling the liquid phase from first-principles is difficult, we simply used the experimentally determined free energy available in the COST light metal database [16]. To ensure that the reference states used in the database and in our calculations are compatible, the free energy of the liquid $G_L(x)$ at a composition of x at % Li was corrected as follows:

$$G_L(x) = G_{L,ex}(x) - (1-x)\, G_{Cu,fcc,ex} - x\, G_{Li,bcc,ex} + (1-x)\, G_{Cu,fcc,fp} + x\, G_{Li,bcc,fp}$$

where the experimental and the first-principles values are denoted by the subscripts "ex" and "fp", respectively.

2.2 Experimental

Galvanic cells using the liquid eutectic mixtures of: LiCl-KCl, LiCl-KCl-CsCl, LiCl-LiF or pure LiCl of the following scheme:

Li (l) / liquid electrolyte containing Li+ ions / Cu-Li (s)

were employed using Cu foil to which Li was coulometrically titrated to change the composition. Emf measurements were performed at temperatures 648K and 885 K and concentrations of Li slightly exceeding 0.6 molar fraction of Li.

3. Results

As shown in Figure 3, there are numerous ground states in this system, although most of them disorder below room temperature and have little practical relevance. The only ground state remaining stable above room temperature is the B32 structure at 50% composition (see Figure 4a)). Due to the limitations of the method used to identify the ground states, we cannot rule out the existence of ordered phases based on other lattices than bcc and fcc.

The B32 structure may appear an unlikely candidate to be so stable since it barely breaks the convex hull. However, as temperature increases, the relative stability of B32 substantially increase, for two reasons:

1. The bcc phases have a larger vibrational entropy than comparable fcc phases, so that B32 becomes favored over fcc-based competing phases as temperature increases.
2. The interatomic interactions in this system allow the B32 phase to accommodate a substantial number of point defects without loosing its long range order. This disorder increases the entropy of the B32 phase and promotes its stability at elevated temperature.

Given the unexpected topology of the calculated phase diagram, a few remarks are in order. Although the presence of a Cu-rich bcc solid solution is surprising, given the assessments of Pelton [15] and of Saunders [16], this phase is consistent with the suggestion of Kraus et al. [19] and Old et al. [20] that a solid phase with about 20 at. % Li may be present. Interestingly, the shape of the fcc phase boundary is qualitatively similar to the one proposed by Pelton, thus indicating that our findings do corroborate some aspects of his assessment.

Another interesting feature is that the 1st order transition between the fcc and bcc phases becomes extremely narrow at the point where it intersect the 2nd order transition between the B32 phase of the Li-rich bcc solid solution. Although, the presence of the B32 phase may be unexpected given the earlier work on the Cu-Li system, such a phase is present in the related Al-Li system [39-41].

The calculated shapes of the liquidus and the solidus exhibit a congruent point at about 18 at % Li, which conflicts with all previous assessments. Such a discrepancy could easily arise due to errors in our calculated free energy of the bcc phase that are within the estimated precision of the method, as quoted in Table 1. Another possibility is that the free energy of mixing of both the

liquid and the solid phases are slightly underestimated in the COST database. As a result, the liquidus and the solidus as predicted by the COST database match the known experimental phase boundaries, but when the liquid thermodynamic data from the COST database is combined with first-principles solid-state thermodynamic data, the bias becomes visible. In any event, this small problem could be easily corrected in a full thermodynamic assessment relying on both first-principle data and experimentally observed solidus-liquidus boundaries.

Verifying whether our thermodynamic model is able to reproduce our emf measurements provides a very sensitive benchmark of the accuracy of the methods employed. As seen in Figure 5a), the calculations compare favorably with the experimental results. To facilitate the comparison, two adjustable parameters were introduced into the calculations. First, since the chemical potential of Li in liquid Li is difficult to calculate from first-principles, it was left as an adjustable parameter and determined so that the vertical position of the plateau in the calculated emf associated with the fcc-bcc two-phase equilibrium matches experimental measurements. Secondly, since first-principles calculations typically suffer systematic biases on the temperature scale, the temperature of the Monte Carlo simulations was also left as an adjustable parameter determined so as to best reproduce the location of the fcc to bcc transition. However, thanks to the inclusion of lattice vibrations in the thermodynamic model, the resulting fitted temperature (950K) is quite close to the actual temperature (885K) at which the measurements were made.

A full thermodynamic assessment of the Cu-Li system would likely include both experimental and first-principles data. To illustrate how well such an optimized thermodynamic model including only one fcc phase, one bcc phase and a B32 phase would reproduce the emf curve, we

slightly adjusted the width of the 1st order transition and the location of the 2nd order transition. These semi-empirically "adjusted" results, shown in Figure 5b) suggest that no other phases are needed to describe the shape of the emf curve at 885K. However, given the accuracy of our calculations, we cannot rule out that the bcc phase may be actually slightly less stable than we have found. This might cause the fcc and the bcc free energy curves to cross 3 times at around 885K, resulting in 3 plateaus in the emf curve, which is also compatible with the experimental measurements. The phase diagram corresponding to this alternative scenario is schematically depicted in Figure 5b).

4. **Conclusion**

Our first-principles calculations and electrochemical measurements suggest that the only stable ordered compound above room temperature is a B32 phase at 50 at % Li, which undergoes a second order phase transition into a bcc solid solution around 900K-1200K, thus indicating that the previously suggested Cu_4Li phase is probably a Cu-rich bcc solid solution (although we cannot entirely rule out the presence of ordered phase that are not superstructures of bcc or fcc). Our results would certainly benefit from further experimental corroboration. For instance, it should be possible to obtain the high-temperature bcc phase or the B32 phase by cooling a liquid solution containing more than 70 at. % Li. The composition of the resulting solid precipitates would be such that the bcc coordination would probably be maintained even after quenching, thus enabling room-temperature X-ray diffraction analysis. The present study illustrates how first-principles calculations can be very helpful in order to clarify the topology of a phase diagram and guide further experimental investigations.

Acknowledgements

This work is supported by the U.S. National Science Foundation under programs DMR-0080766 and DMR-0076097 and by the U.S. Department of Energy under contract no. DE-F502-96ER 45571.

References

1. J.F.Smith and Z.Moser, J.Nucl.Mater. 59 (1976) 158.
2. Z.Moser, W.Gąsior, F.Sommer, G.Schwitzgebel and B.Predel, Met.Trans.B 17 (1986) 791.
3. Z.Moser, F.Sommer and B.Predel, Z.Metallkde. 79 (1988) 705.
4. Z.Moser, F.Sommer, J.J.Lee and B.Predel, Thermochim.Acta 142 (1989) 117.
5. W.Gąsior and G.Schwitzgebel, Archs. of Metallurgy 37 (1992) 25.
6. W.Gąsior and Z.Moser. J.Chem.Phys. 90 (1993) 387.
7. W.Gąsior, G.Schwitzgebel and H.Ruppersberg, Archs. of Metallurgy 39 (1994) 25.
8. W.Gąsior, Z.Moser and W.Zakulski, J.Non-Crystalline Solids 205-207 (1996) 379.
9. W.Gąsior, Z.Moser and W.Zakulski. Archs. of Metallurgy 39 (1994) 356.
10. W.Gąsior, Z.Moser, W.Zakulski and G.Schwitzgebel, Mater.Met.Trans.A 27 (1996) 2419.
11. W. Gąsior, Z.Moser, J. Nucl. Mater. 249, (2001) 77-83.
12. Z. Moser, R.Agarwal, F.Sommer and B.Predel, Z.Metallkde. 82 (1991) 317.
13. Z. Moser, W.Gąsior, F.Sommer, W.Zakulski, H.J.Seifert and H.L.Lukas, CALPHAD XXIV, Kyoto, Japan, 21-26 May 1995. Program and Abstracts, p.29.
14. W. Gąsior, Z.Moser, B.Onderka, F.Sommer and B.Kim, Proceedings of 10th International IUPAC Conference on High Temperature Materials Chemistry, 10-14 April 2000, Jülich,Germany.
15. A.D. Pelton, Bull. Alloy Phase Diagrams, 7, (1986) 142.
16. N. Saunders, COST 537 Thermochemical database for light metal alloys, Vol.2, Ed. I. Ansara, A.T. Dindail, M.H. Rand, European Communities, 1998, p. 168.
17. Borgsttedt, Gumiński, "Metals in Liquid Alkali Metals", Solubility Data Series, vol. 64, Oxford University Press, oxford, 1996, p. 59
18. M.V Mikhailovskaya, V.S. Sudavtsova, Ukr. Khim.Zh., 55 (1989) 1106.
19. A.R.Krauss, M.H.Mendelson, D.M.Gruen, R.W.Coon, D.M.Goebel, Y.Hiroaka, W.K.Leung, J.Bohdanowsky, J. US Dep.Ener.Rep. CONF-86-0807-3, 1986.

20. C.F.Old, P.Trawena, Met.Sci, 15,(1981) 281.
21. A.R.Miedema, F.R.de Boer and R.Boom, CALPHAD, 1, (1977) 314.
22. A. van de Walle, M. Asta and G. Ceder, *CALPHAD Journal*, 26, 539 (2002).
23. A. van de Walle and G. Ceder, *Journal of Phase Equilibria*, 23:348, 2002.
24. A. van de Walle and M. Asta, *Modelling Simul. Mater. Sci. Eng.,* 10:521, 2002.
25. G. Kresse and J. Furthmüller, *Phys. Rev. B* 54, 11169 (1996).
26. G. Kresse and J. Furthmüller, *Comp. Mat. Sci.* 6, 15 (1996).
27. J. M. Sanchez, F. Ducastelle and D. Gratias, *Physica* 128*A*, 334 (1984).
28. F. Ducastelle, *Order and Phase Stability in Alloys*. Elsevier Science, New York, (1991).
29. D. de Fontaine, *Solid State Phys.* 47, 33 (1994).
30. A. Zunger. First principles statistical mechanics of semiconductor alloys and intermetallic compounds. In P. E. Turchi and A. Gonis, editors, *NATO ASI on Statics and Dynamics of Alloy Phase Transformation*, volume 319, page 361, Plenum Press, New York (1994).
31. M. Asta, V. Ozolins and C. Woodward, *Journal of the Minerals Metals & Materials Society*, 53, 16 (2001).
32. G. Ceder and A. van der Ven and C. Marianetti and D. Morgan, *Modelling Simul. Mater. Sci. Eng.*, 8, 311 (2000).
33. A. A. Maradudin and E. W. Montroll and G. H. Weiss, *Theory of Lattice Dynamics in the Harmonic Approximation*, Second Edition, Academic Press, New York (1971).
34. A. van de Walle and G. Ceder, *Rev. Mod. Phys.*, 74, 11 (2002).
35. G. Ceder, *Comput. Mater. Sci.* 1, 144 (1993).
36. E. Wu, G. Ceder and A. van de Walle, *Phys. Rev. B*, 67, 134103 (2003).
37. K. Binder and D. W. Heermann, *Monte Carlo Simulation in Statistical Physics*. Springer-Verlag, New York (1988).
38. M. E. J. Newman and G. T. Barkema, *Monte Carlo Methods in Statistical Physics*, Clarendon Press, Oxford (1999).
39. M. L. Saboungi and C.C. Hsu, *Calphad* 1, 237 (1977).
40. A.J. McAlister, *Bull. Alloy Phase Diagrams* 3, 177-1982.
41. M. H. F. Sluiter, Y. Watanabe, D. de Fontaine and Y. Kawazoe, Phys. Rev. B, 53, 6137 (1996), and references therein

Table 1

Lattice	fcc	bcc
Number of structures	41	35
Number of clusters*	8+12+1	5+13
Cross-validation score (meV)	3.9	33

*The number of cluster is reported as the number of pairs, triplets, etc.

Figure 1

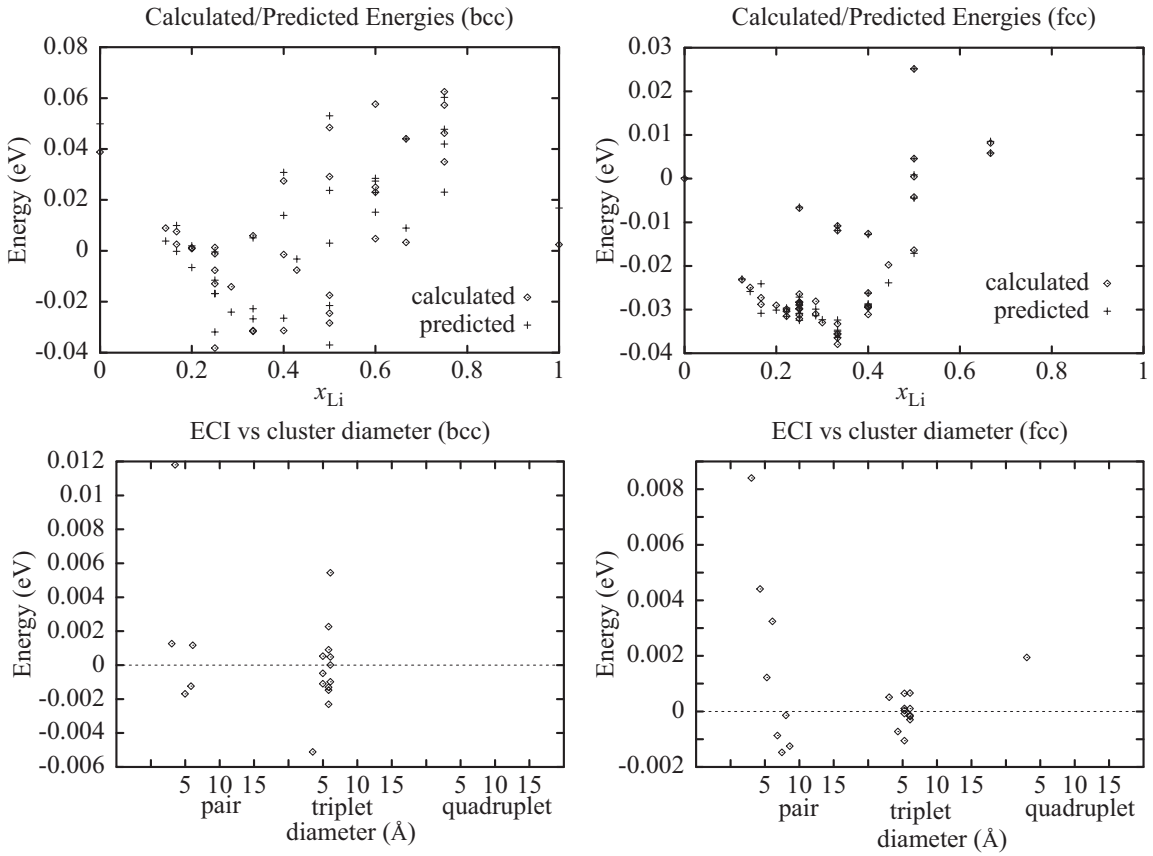

Figure 2

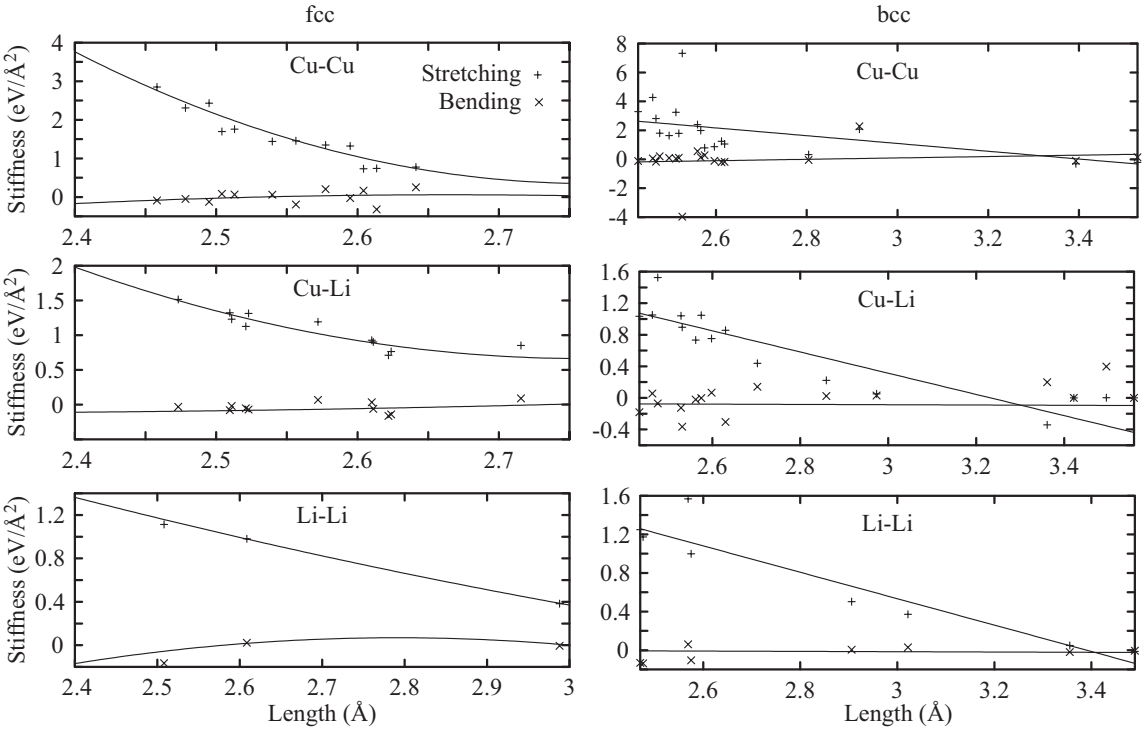

Figure 3

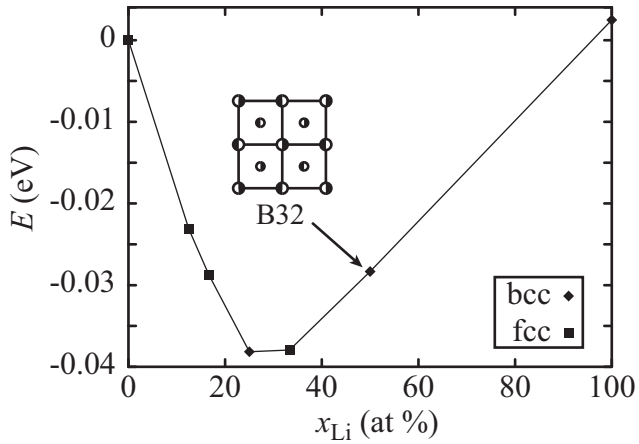

Figure 4

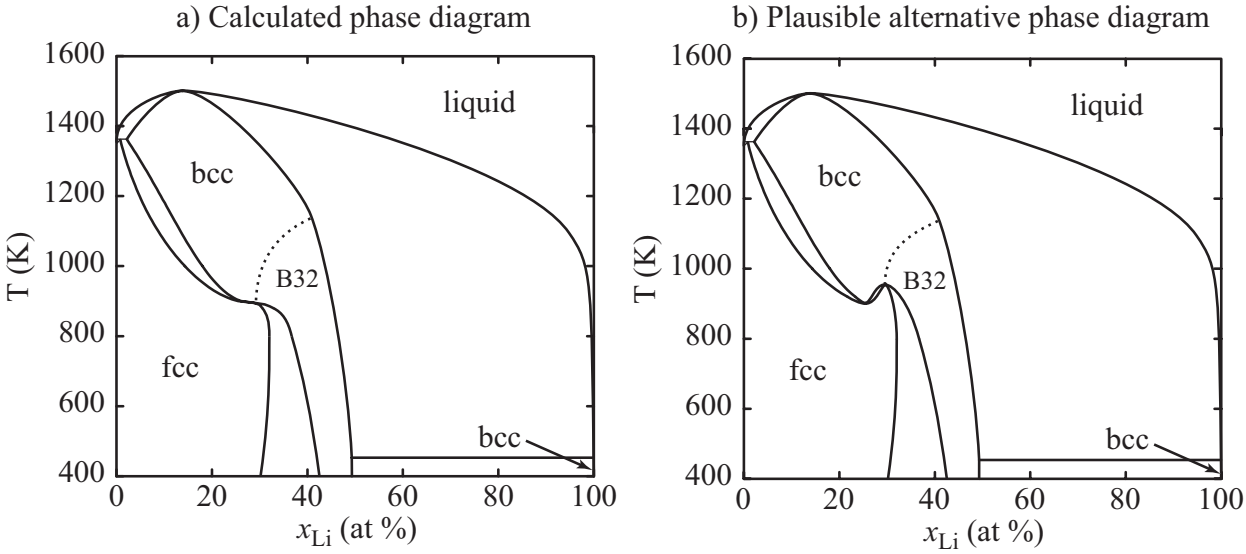

Figure 5

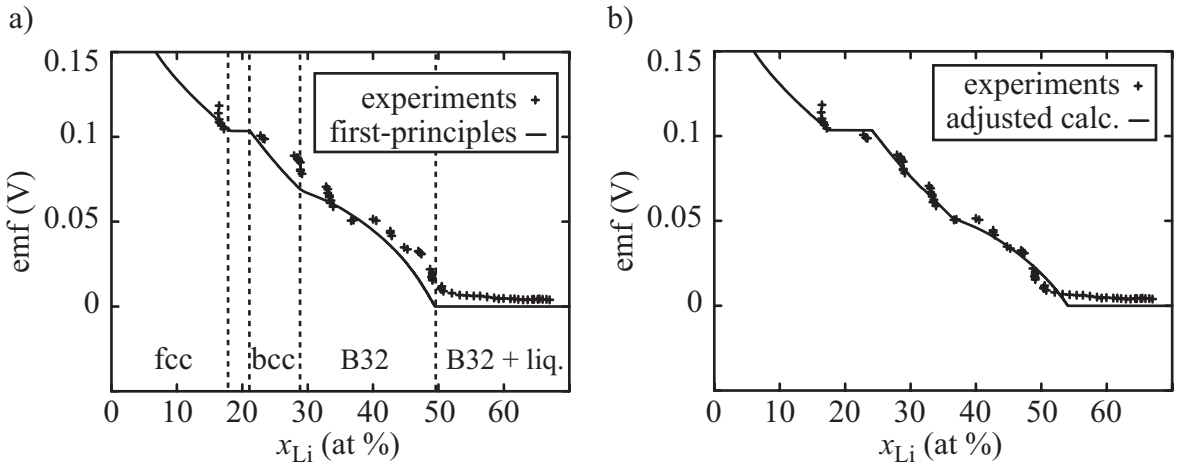

Table 1: Characteristics of the cluster expansion used.

Figure 1: Database of first-principles energies (top) used to determine the ECI (bottom).

Figure 2: Determination of the Length-Dependent Force Constants.

Figure 3: Ground states of the Cu-Li system.

Figure 4: Cu-Li phase diagram.

Figure 5: Calculated and measured emf curves.